

THE EFFECTS OF DIFFERENT ENGINE MATERIAL PROPERTIES ON THE PERFORMANCE OF A DIESEL ENGINE AT MAXIMUM COMBUSTION TEMPERATURES

*Yuksel PALACI, Guven GONCA**

Yildiz Technical University, Naval Arch. and Marine Eng. Depart, Besiktas, Istanbul, TR

In this study, the influences of various engine materials such as palladium, titanium, thorium, zirconium, vanadium, alumina, aluminum bronze, copper, iron (Gray cast), manganese, nickel, cobalt, carbon steel on the effective efficiency and effective power with respect to the variation of equivalence ratio at the maximum combustion temperatures. In-cylinder gas temperatures have been determined with respect to the melting temperatures and the performance values have been calculated with respect to the variation of the gas temperatures. The results indicated that alumina provides the maximum performance values as aluminum bronze gives the minimum performance values due to the combustion temperatures. Furthermore, the equivalence ratios which give the maximum performance characteristics have been parametrically described. The obtained results can be assessed by engine designers and manufacturers to choose suitable engine material.

Key words: engine material; performance, combustion temperatures; diesel engine; equivalence ratio

1. Introduction

Diesel engines and marine diesel engines are the most common devices utilized in the transportation sectors. There are so many optimization works on the Diesel engines. Xia et al. [1] examined the performance of a diesel engine cycle to optimize the piston motions and to make better thermal efficiency and net work. Hinti et al. [2] used an alternative calculation for heat transfer loss to analysis performance of an air-standard diesel engine cycle. Sakhrieh et al. [3] used a novel gas mixture model in a zero-dimensional simulation model to examine the performance characteristics of a diesel engine cycle. Acikkalp and Caner [4] analyzed a nano scale irreversible dual cycle by using Ideal Maxwell–Boltzmann gas constant for working fluid. Acikkalp and Caner [5] used different thermodynamic assessment methods to compare the performance of a nano scale irreversible dual cycle engine operating with ideal Bose and Fermi gases. Ge et al. [6] used finite time thermodynamics methods to analyze the performance of an air standard dual cycle engine and they compared the performances of diesel, otto and dual cycle engines. Hou [7] examined the impacts of heat transfer loss on the performance specifications of a dual cycle engine. Ust et al. [8] expanded prior study for an irreversible dual cycle engine. Gonca and Sahin [9] analyzed the performance specifications of a hydrogen-enriched diesel engine with steam injection technique. Gonca [10] and Gonca et al. [11-16] performed a couple of studies on the Miller cycle Diesel engines and steam-injected Diesel engines. Li et al. [17] decreased pollutant emissions simultaneously using an effective approach and it was expressed that premixed natural gas has a positive correlation with power output. Acikkalp et al. [18]

analyzed a diesel-gas engine trigeneration system in Turkey by using exergy analysis. Vellaiyan and Amirthagadeswaran [19] optimized operating parameters of a diesel engine operating with diesel-water emulsion fuel. Liu et al. [20] examined the impacts of injection timing and EGR combinations on the combustion characteristics and particulate matter emission of a diesel engine operating on ethanol-diesel blends.

Although there are so many thermodynamic optimization works for the Diesel engines, material researches are insufficient. Novel advanced material technologies must be developed by the scientists for engine manufacturing by considering cost and environmental restrictions. In this report, the influences of structure materials of the diesel engines such as palladium, titanium, thorium, zirconium, vanadium, alumina, aluminum bronze, copper, iron (Gray cast), manganese, nickel, cobalt and carbon steel on the performance characteristics have been parametrically examined with respect to the equivalence ratio variation. There is not any study in the literature investigating the different material properties on the engine performance of the diesel engines. This study considers engine material properties and engine operating conditions altogether. Therefore, it is very important to make up for the deficiency in this field.

2. Theoretical model

This study carried out a performance examination for a dual cycle based diesel engine which is constructed with different engine materials. The cycle is shown in Fig. 1. Maximum melting temperatures of materials used for engine manufacturing are demonstrated in Table 1.

Table 1. Maximum Melting point of materials used for engine manufacturing [34]

Material	Maximum Melting point (°C)
Palladium	1555
Titanium	1670
Thorium	1750
Zirconium	1854
Vanadium	1900
Alumina	2072
Aluminum bronze	1038
Copper	1084
Gray cast iron	1204
Manganese	1244

Nickel	1453
Cobalt	1495
Carbon steel	1540

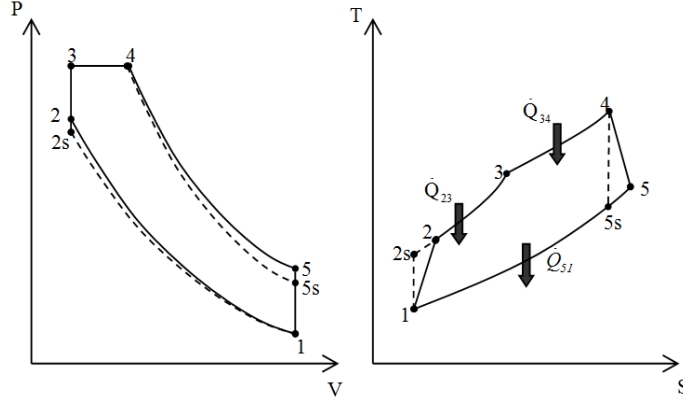


Fig. 1. P-v and T-s diagrams for the irreversible Dual-Diesel cycle

A numerical simulation of engine efficiency and power is performed. In the study, air intake pressure (p_1), intake temperature (T_1), engine speed (N), cycle temperature ratio (α), cylinder stroke length (L), bore diameter (d), residual gas fraction (RGF), cylinder wall temperature (T_w) and friction coefficient (μ) are considered in calculations and they are defined as follows; 100 kPa, 300 K, 3600 rpm, 8, 0.072 m, 0.062 m, 0.05, 400 K and 12.9 Ns/m, respectively, at the first condition. The effective efficiency and power can be expressed as follows:

$$P_{ef} = \dot{Q}_{in} - \dot{Q}_{out} - P_l, \eta_{ef} = \frac{P_{ef}}{\dot{Q}_f} \quad (1)$$

Where, the heat addition (\dot{Q}_{in}) at constant volume (2-3) and constant pressure (3-4), the heat rejection (\dot{Q}_{out}) at constant volume (5-1) and loss power by friction (P_l) [11] can be given as follows:

$$\dot{Q}_{in} = \dot{Q}_{f,c} - \dot{Q}_{ht} = \dot{m}_T \left[\int_{T_2}^{T_3} C_V dT + \int_{T_3}^{T_4} C_p dT \right] = \dot{m}_T \left(\left[\left(\left[\left(2.506 \cdot 10^{-11} \frac{T^3}{3} + 1.454 \cdot 10^{-7} \frac{T^{2.5}}{2.5} - 4.246 \cdot 10^{-7} \frac{T^2}{2} + 3.162 \cdot 10^{-5} \frac{T^{1.5}}{1.5} + 1.0433T - 1.512 \cdot 10^4 \left(-\frac{T^{-0.5}}{0.5} \right) + 3.063 \cdot 10^5 (-T^{-1}) - 2.212 \cdot 10^7 \left(-\frac{T^{-2}}{2} \right) \right]_{T_2}^{T_3} \right) + \left(\left[\left(2.506 \cdot 10^{-11} \frac{T^3}{3} + 1.454 \cdot 10^{-7} \frac{T^{2.5}}{2.5} - 4.246 \cdot 10^{-7} \frac{T^2}{2} + 3.162 \cdot 10^{-5} \frac{T^{1.5}}{1.5} + 1.3301T - 1.512 \cdot 10^4 \left(-\frac{T^{-0.5}}{0.5} \right) + 3.063 \cdot 10^5 (-T^{-1}) - 2.212 \cdot 10^7 \left(-\frac{T^{-2}}{2} \right) \right]_{T_3}^{T_4} \right) \right] \right) \quad (2)$$

$$\dot{Q}_{out} = \dot{m}_T \int_{T_1}^{T_5} C_v dT = \left[\dot{m}_T \left(2.506 \cdot 10^{-11} \frac{T^3}{3} + 1.454 \cdot 10^{-7} \frac{T^{2.5}}{2.5} - 4.246 \cdot 10^{-7} \frac{T^2}{2} + 3.162 \cdot 10^{-5} \frac{T^{1.5}}{1.5} + 1.0433T - 1.512 \cdot 10^4 \left(-\frac{T^{-0.5}}{0.5} \right) + 3.063 \cdot 10^5 (-T^{-1}) - 2.212 \cdot 10^7 \left(-\frac{T^{-2}}{2} \right) \right) \right]_{T_1}^{T_5} \quad (3)$$

$$P_l = \mu c_m^2 = \frac{\left[Z + 48 \left(\frac{N}{1000} \right) + 0.4 c_m^2 \right] V_s N}{1200} \quad (4)$$

The other equations have been obtained from ref. [21]. Where Z is a constant which is related to friction [11] and its is 75, where μ is friction coefficient, c_m is average piston velocity which is written as follows:

$$c_m = \frac{S \cdot N}{30} \quad (5)$$

Where S is stroke (m) and N is engine speed (rpm). \dot{Q}_f states heat potential of the fuel injected into the cylinder and it is derived as follows:

$$\dot{Q}_f = \dot{m}_f H_u \quad (6)$$

Where H_u is calorific value of the fuel. \dot{m}_f signifies mass flow rate of fuel per second and it is expressed as below:

$$\dot{m}_f = \frac{m_f N}{120} \quad (7)$$

$\dot{Q}_{f,c}$ signifies heat release and \dot{Q}_{ht} is the heat loss by heat transfer into cylinder wall and they are given as below:

$$\dot{Q}_{f,c} = \eta_c \dot{m}_f H_u \quad (8)$$

$$\dot{Q}_{ht} = h_{tr} A_{cyl} (T_{me} - T_w) = h_{tr} A_{cyl} \left(\frac{T_2 + T_3}{2} - T_w \right) \quad (9)$$

Where, η_c expresses efficiency of the combustion process. It is stated as follows [22-24]:

$$\eta_c = -1.44738 + \frac{4.18581}{\phi} - \frac{1.86876}{\phi^2} \quad (10)$$

ϕ expresses equivalence ratio and it could be given as:

$$\phi = \frac{(m_f / m_a)}{F_{st}} \quad (11)$$

Where, m_a signifies the mass of the air per cycle (kg) introduced into the cylinder during the intake process. F_{st} expresses ratio of the fuel and air at stoichiometric combustion conditions. They are written as below:

$$m_a = \rho_a V_a = \rho_a (V_T - V_{rg}) \quad (12)$$

$$V_T = V_s + V_c = \frac{(V_s r)}{r-1} \quad (13)$$

$$V_c = \frac{V_T}{r} = \frac{\pi d^2 S}{4} \frac{1}{r-1} \quad (14)$$

$$F_{st} = \frac{\varepsilon \cdot (12.01 \cdot \alpha + 1.008 \cdot \beta + 16 \cdot \gamma + 14.01 \cdot \delta)}{28.85} \quad (15)$$

$$\rho_a = f(T_1, P_1) \quad (16)$$

Where V_c , V_a , V_s , V_{rg} and V_T are volumes of compression, air, stroke, residual gas and total cylinder.

ρ_{rg} is residual gas density which is expressed as follows:

$$\rho_{rg} = f(T_{mix}, P_1) \quad (17)$$

T_{mix} is mean temperature of air-residual gas mixtures which is states as follows:

$$T_{mix} = \frac{\dot{m}_a T_a R_a + \dot{m}_{rg} T_{rg} R_{rg}}{\dot{m}_a R_a + \dot{m}_{rg} R_{rg}} \quad (18)$$

R_a signifies gas constant of the air, which is 0.287 kJ/kg.K and R_{rg} signifies gas constant of the residual gas, which is 0.293 kJ/kg.K. The compression ratio (r) of the engine is [25-28]:

$$r = V_1 / V_2 \quad (19)$$

The functional statements are acquired by using Engineering Equation Solver [29]. The used fuel in the combustion model is diesel ($C_{14.4}H_{24.9}$) [30]. ε signifies molar ratio of the fuel to air [31]:

$$\varepsilon = \frac{0.21}{\left(\psi - \frac{\gamma}{2} + \frac{\beta}{4} \right)} \quad (20)$$

ψ expresses carbon atom number, β expresses hydrogen atom number and γ oxygen atom number in the used fuel. h_{tr} is coefficient for the heat transfer and it is given as follows [32]:

$$h_{tr} = 130 V_T^{-0.06} P_1^{0.8} T_{mix}^{0.4} (c_m + 1.4)^{0.8} \quad (21)$$

Where A_{cyl} is the heat transfer area (m^2). \dot{m}_a , \dot{m}_{rg} , \dot{m}_T and are flow rates (kg/s) of air, residual-gas and total charge which are stated as follows:

$$\dot{m}_T = \dot{m}_a + \dot{m}_f + \dot{m}_{rg}, \quad (22)$$

$$\dot{m}_a = \frac{m_a N}{120} = \frac{\dot{m}_f F_{st}}{\phi}, \quad (23)$$

$$\dot{m}_{rg} = \frac{m_{rg} N}{120} = \dot{m}_a RGF, \quad (24)$$

$$A_{cyl} = \pi d S \frac{r}{r-1} + \frac{\pi d^2}{2} \quad (25)$$

Where m_a signifies the mass of the air per cycle (kg), m_{rg} signifies the mass of the residual-gas per cycle (kg). RGF means residual-gas fraction. T_w and T_{me} are cylinder wall temperature and average combustion temperature. C_V and C_P are constant volume and constant pressure specific heats which are stated as follows [32,35]:

$$C_p = 2.506 \cdot 10^{-11} T^2 + 1.454 \cdot 10^{-7} T^{1.5} - 4.246 \cdot 10^{-7} T + 3.162 \cdot 10^{-5} T^{0.5} + 1.3301 - 1.512 \cdot 10^4 T^{-1.5} + 3.063 \cdot 10^5 T^{-2} - 2.212 \cdot 10^7 T^{-3} \quad (26)$$

$$C_V = C_P - R \quad (27)$$

The relations for (1-2s) process and (4-5s) process are attained as below [33]:

$$C_{V_1} \cdot \ln \left| \frac{T_{2s}}{T_1} \right| = R \ln |r|, C_{V_2} \cdot \ln \left| \frac{T_{5s}}{T_4} \right| = R \cdot \ln \left| \frac{1}{r} \right| \quad (28)$$

3. Results and discussion

Figs. 2-3 show the equivalence ratios (ϕ) and different engine materials on the effective power. The maximum effective power enhances with raising melting point also the melting points of the materials enhance from palladium to alumina. Alumina provides maximum effective power as it has the maximum melting temperature. However, aluminum bronze has the minimum effective power since it has the minimum melting temperature. The melting temperature of the materials increases from aluminum bronze to carbon steel as can be observed in the Fig. 2. However, the ϕ affects the engine power, it augments with enhancing ϕ to a specified point and then starts to diminish with enhancing ϕ . The optimum equivalence ratio which gives the maximum engine power shifts right with respect to increasing melting temperatures. This result has been observed from aluminum bronze to carbon steel and from palladium to alumina in both of the figures.

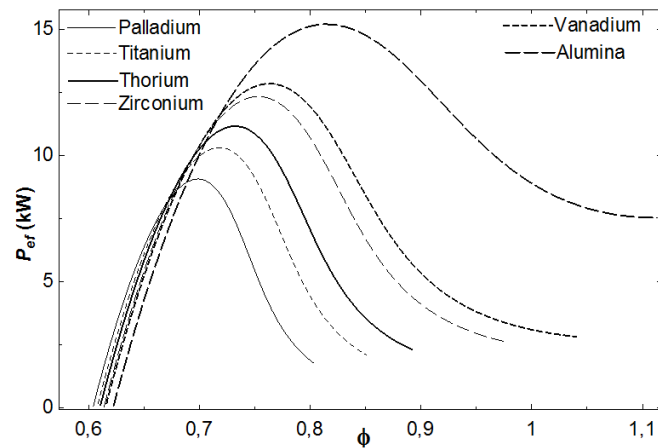


Fig. 2. The effects of equivalence ratios and different engine materials which have high melting temperatures on the effective power

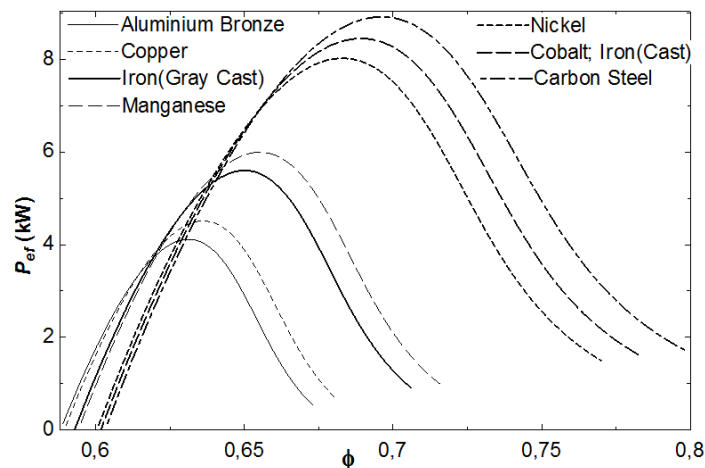


Fig. 3. The effects of equivalence ratios and different engine materials which have low melting temperatures on the effective power

Figs 4-5 show the equivalence ratios and different engine materials on the effective efficiency with respect to the equivalence ratio. It is clear that the maximum effective efficiency increases with

increasing maximum melting temperatures. The maximum engine efficiency is obtained with alumina while the minimum effective power is attained with aluminum bronze as the maximum melting temperatures of the materials studied rises from aluminum bronze to alumina. However, the efficiency is affected by the ϕ . The engine efficiency first enhances with increasing equivalence ratio to a determined value and then begins to reduce with enhancing ϕ . The optimum ϕ which provides the maximum effective efficiency shifts right with respect to enhancing melting temperatures. It increases from aluminum bronze to alumina.

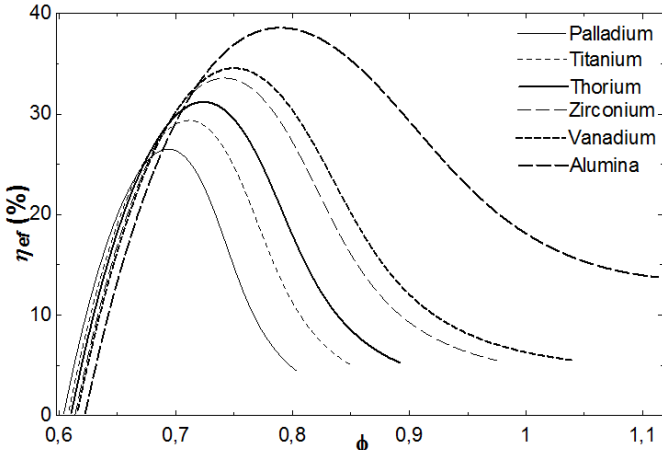


Fig. 4. The effects of equivalence ratios and different engine materials which have high melting temperatures on the effective efficiency

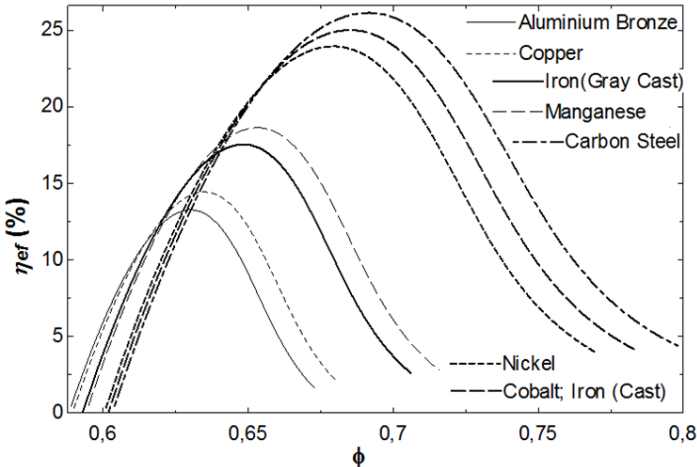


Fig. 5. The effects of equivalence ratios and different engine materials which have low melting temperatures on the effective efficiency

Figs 6-7 show the variation of the engine power and efficiency with respect to the variation of the ϕ and different engine materials. The engine power and efficiency enhance altogether with changing materials. Aluminum bronze provides the minimum power and efficiency as it has the minimum melting temperature. However, the maximum performance characteristics are obtained with alumina.

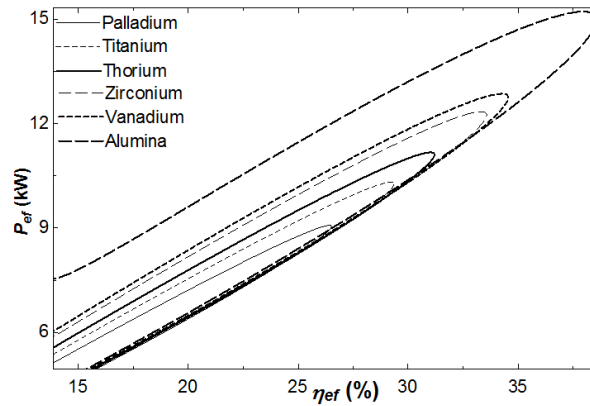


Fig. 6. The variation of the effective power and effective efficiency at the different engine materials which have high melting temperatures

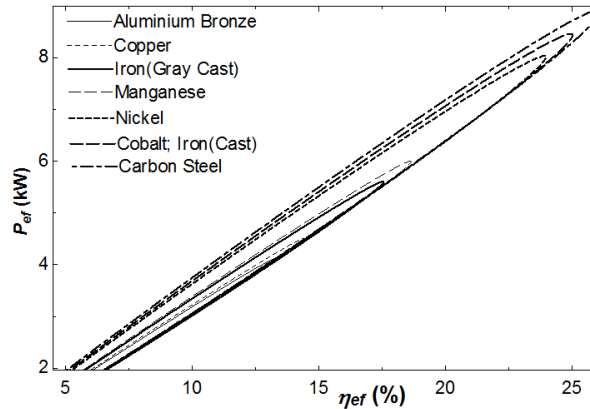


Fig. 7. The variation of the effective power and effective efficiency at the different engine materials which have high melting temperatures

In exceptional running conditions, when cylinder walls have a cooling system problem occurs, cylinder walls may reach the gas temperature at the specific location of the inner surface. This will cause melting and material deformation at this specific locations. The engine material can fail in a short time with hot deformation and wear. The material can fail under load which may be lower than yield strength of the material at high temperatures as a well known creep phenomena. As a conclusion, the maximum temperature of combustion gas can be taken as a melting temperature of the cylinder wall to avoid damage on the cylinder walls as an approach to possible cooling problem.

4. Conclusion

This work reports the effects of engine structure materials such as palladium, titanium, thorium, zirconium, vanadium, alumina, aluminum bronze, copper, iron (Gray cast), manganese, nickel, cobalt, carbon steel on the performance characteristics with respect to the equivalence ratio variation. The results showed that the maximum engine power and efficiency enhance with augmenting melting points. Therefore, while the alumina provides the maximum performance characteristics, aluminum bronze has the minimum performance characteristics due to melting temperatures. Moreover, the equivalence ratio has a considerable impact on the performance characteristics. They augment with raising equivalence ratio to a particular value and then start to diminish with increasing equivalence ratio. The optimum equivalence ratio which provides the maximum performance characteristics shifts

right with respect to increasing melting temperatures. It increases from palladium to alumina. This study has a remarkable originality and it can be used as an approach by engine manufacturers and designers..

Acknowledgment

The authors thank Turkish Academy of Sciences (TUBA) for financial supporting.

References

- [1] Xia, S., *et al.*, Engine performance improved by controlling piston motion: Linear phenomenological law system Diesel cycle, *International Journal of Thermal Sciences*, 51 (2012), 1, pp. 163-174
- [2] Al-Hinti, I., *et al.*, Performance analysis of air-standard Diesel cycle using an alternative irreversible heat transfer approach, *Energy Convers. Manage.*, 49 (2008), 11, pp. 3301–3304
- [3] Sakhrieh, A., *et al.*, Performance of a diesel engine using a gas mixture with variable specific heats model, *J Energy Inst.*, 83 (2010), 1, pp. 217–224
- [4] Acikkalp, E., Caner, N., Determining performance of an irreversible nano scale dual cycle operating with Maxwell–Boltzmann gas, *Physica A*, 424 (2015), 1, pp. 342–349
- [5] Acikkalp, E., Caner, N., Determining of the optimum performance of a nano scale irreversible Dual cycle with quantum gases as working fluid by using different methods, *Physica A*, 433 (2015), 1, pp. 247–258
- [6] Ge, Y., *et al.*, Finite-time thermodynamic modeling and analysis for an irreversible Dual cycle, *Mathematical and Computer Modelling*, 50 (2009), 1, pp. 101-108
- [7] Hou, S.S., Heat Transfer Effects on the Performance of an Air Standard Dual Cycle, *Energy Convers. Manage.*, 45 (2004), 18, pp. 3003–3015
- [8] Ust, Y., *et al.*, Heat Transfer Effects on the Performance of an Air –Standard Irreversible Dual Cycle, *International Journal of Vehicle Design*, 63 (2013), 1, pp. 102–116
- [9] Gonca, G., Sahin, B., Simulation of Performance and Nitrogen Oxide Formation of a Hydrogen-Enriched Diesel Engine with the Steam Injection Method, *Thermal Science*, 19 (2015), 6, pp. 1985-1994
- [10] Gonca, G., Thermo-Ecological Analysis of Irreversible Dual-Miller Cycle (DMC) Engine Based on the Ecological Coefficient of Performance (ECOP) Criterion, *Iran J. Sci. Technol. Trans. Eng.*, 41 (2017), 41, pp. 269-280
- [11] Gonca, G., *et al.*, A Study on Late Intake Valve Closing Miller Cycled Diesel Engine, *Arab J Sci Eng.*, 38 (2013), 1, pp. 383-93
- [12] Gonca, G., *et al.*, Performance maps for an air-standard irreversible Dual-Miller cycle (DMC) with late inlet valve closing (LIVC) version, *Energy*, 5 (2013), 1, pp. 285-290
- [13] Gonca, G., *et al.*, Investigation of Heat Transfer Influences on Performance of Air-Standard Irreversible Dual-Miller Cycle, *Journal of Thermophysics and Heat Transfer*, 29 (2013), 4, pp. 678-683

- [14] Gonca, G., *et al.*, Theoretical and Experimental Investigation of the Miller Cycle Diesel Engine in Terms of Performance and Emission Parameters, *Applied Energy*, 138 (2015), 4, pp. 11-20
- [15] Gonca, G., *et al.*, Comparison of Steam Injected Diesel Engine and Miller Cycled Diesel Engine By Using Two Zone Combustion Model, *Journal of the Energy Institute*, 88 (2015), 1, pp. 43-52
- [16] Gonca, G., *et al.*, The Effects of Steam Injection on the Performance and Emission Parameters of a Miller Cycle Diesel Engine, *Energy*, 78 (2014), 1, pp. 266-275
- [17] Li, J., *et al.*, Adjusting the operating characteristics to improve the performance of an emulsified palm oil methyl ester run diesel engine, *Energy Convers. Manage.*, 69 (2013), 11, pp. 191-198
- [18] Acikkalp, E., *et al.*, Advanced exergoeconomic analysis of a trigeneration system using a diesel-gas engine, *Applied Thermal Engineering*, 67 (2014), 1-2, pp. 388-395
- [19] Vellaiyan, S., Amirthagadeswaran K.S.N, Multi-Response Optimization of Diesel Engine Operating Parameters Running with Water-In-Diesel Emulsion Fuel, *Thermal Science*, 21 (2017), 1, pp. 427-439
- [20] Liu, J., *et al.*, The Effects of EGR and Injection Timing on The Engine Combustion And Particulate Matter Emission Performances Fuelled With Diesel-Ethanol Blends, *Thermal Science*, 22 (2018), 3, pp. 1457-1467
- [21] Gonca, G., Thermodynamic analysis and performance maps for the irreversible Dual-Atkinson cycle engine (DACE) with considerations of temperature-dependent specific heats, heat transfer and friction losses, *Energy Convers. Manage.*, 111 (2016), 1, pp. 205-216
- [22] Ebrahimi, R., Performance analysis of an irreversible Miller cycle with considerations of relative air-fuel ratio and stroke length, *Applied Mathematical Modelling*, 36 (2012), 1, pp. 4073-4079
- [23] Ebrahimi, R., Thermodynamic modeling of performance of a Miller cycle with engine speed and variable specific heat ratio of working fluid, *Computers and Mathematics with Applications*, 62 (2011), 1, pp. 2169-2176
- [24] Ebrahimi, R., Effects of mean piston speed, equivalence ratio and cylinder wall temperature on performance of an Atkinson engine, *Mathematical and Computer Modelling*, 53 (2011), 1, pp. 1289-1297
- [25] Rashidi, M.M., Hajipour, A., Comparison of Performances of Air-Standard Atkinson, Diesel and Otto Cycles with Constant Specific Heats, *Int J Advanced Design and Manufacturing Technology*, 6 (2013), 1, pp. 57-62
- [26] Rashidi, M.M., *et al.*, First and Second-Law Efficiency Analysis and ANN Prediction of a Diesel Cycle with Internal Irreversibility, Variable Specific Heats, Heat Loss, and Friction Considerations, *Advances in Mechanical Engineering*, 359872 (2014), 1, pp. 1-16
- [27] Rashidi, M.M., *et al.*, First and Second-Laws Analysis of an Air-Standard Dual Cycle With Heat Loss Consideration, *International Journal of Mechatronics, Electrical and Computer Technology*, 4 (2014), 1, pp. 315-332

- [28] Mousapour, A., *et al.*, Performance evaluation of an irreversible Miller cycle comparing FTT (finite-time thermodynamics) analysis and ANN (artificial neural network) prediction, *Energy*, 94 (2016), 1, pp. 100-109
- [29] EES Academic Professional Edition, (2017), V.10.305-3D, USA, F-Chart Software
- [30] Ferguson, C.R., *Internal combustion engines – applied thermosciences*, John Wiley and Sons Inc., New York, USA, 1986
- [31] Hohenberg, G., Advanced Approaches for Heat Transfer Calculations, *SAE 790825* (1979), 1, pp. 1-19
- [32] Ge, Y., *et al.*, Finite-Time Thermodynamic Modelling and Analysis of an Irreversible Otto-Cycle, *Applied Energy*, 85 (2008), 1, pp. 618-624
- [33] Lin, J., *et al.*, Finite-Time Thermodynamic Performance of a Dual Cycle, *Int J Energy Res.*, 23 (1999), 9, pp. 765–772.
- [34] http://www.engineeringtoolbox.com/melting-temperature-metals-d_860.html
- [35] Gonca, G., Palaci, Y., Performance investigation of a Diesel engine under effective efficiency-power-power density conditions, *Scientia Iranica*, (In press.)